Volume 12
Number 17
7 May 2024
Pages 4055–4280

Journal of Materials Chemistry B

Materials for biology and medicine

rsc.li/materials-b

ISSN 2050-750X

ROYAL SOCIETY OF CHEMISTRY

PAPER

Koji Miki, Kouichi Ohe *et al.*

Light-controllable cell-membrane disturbance for intracellular delivery

Journal of Materials Chemistry B

ROYAL SOCIETY OF CHEMISTRY

PAPER

View Article Online
View Journal | View Issue

Cite this: J. Mater. Chem. B, 2024, 12, 4138

Light-controllable cell-membrane disturbance for intracellular delivery†

Wenting Huo,[a] Koji Miki,*[a] Huiying Mu,[a] Takashi Osawa,[b] Harumi Yamaguma,[c] Yuuya Kasahara,[c] Satoshi Obika,[bd] Yoshimasa Kawaguchi,[e] Hisaaki Hirose,[e] Shiroh Futaki,[e] Yusuke Miyazaki,[f] Wataru Shinoda,[f] Shuji Akai[b] and Kouichi Ohe*[a]

Received 15th December 2023,
Accepted 1st March 2024

DOI: 10.1039/d3tb02956e

rsc.li/materials-b

Highly polar and charged molecules, such as oligonucleotides, face significant barriers in crossing the cell membrane to access the cytoplasm. To address this problem, we developed a light-triggered twistable tetraphenylethene (TPE) derivative, **TPE-C-N**, to facilitate the intracellular delivery of charged molecules through an endocytosis-independent pathway. The central double bond of TPE in **TPE-C-N** is planar in the ground state but becomes twisted in the excited state. Under light irradiation, this planar-to-twisted structural change induces continuous cell membrane disturbances. Such disturbance does not lead to permanent damage to the cell membrane. **TPE-C-N** significantly enhanced the intracellular delivery of negatively charged molecules under light irradiation when endocytosis was inhibited through low-temperature treatment, confirming the endocytosis-independent nature of this delivery method. We have successfully demonstrated that the **TPE-C-N**-mediated light-controllable method can efficiently promote the intracellular delivery of charged molecules, such as peptides and oligonucleotides, with molecular weights ranging from 1000 to 5000 Da.

Introduction

Biologically active macromolecules such as peptide drugs[1,2] and oligonucleotide-based pharmaceuticals[3–7] hold tremendous promise for the treatment of a wide range of diseases, such as hepatitis, diabetes, cancer, and metabolic diseases. However, these polar and charged macromolecules face significant challenges in penetrating the cell membrane (plasma membrane) and accessing to the cytoplasm. The phospholipid bilayer structure of the cell membrane restricts the diffusion to only nonpolar small molecules, while polar and charged molecules cannot readily diffuse through the cell membrane.[8] Molecules that are unable to directly penetrate the cell membrane can still be delivered to cells by endocytosis. Various lipid-based[9,10] and polymer-based[11] nanoparticles have been employed in drug delivery systems *via* the endocytosis-dependent pathway. In this case, endocytosed cargo remains in the topological extracellular space. To release drugs into the cytoplasm, nanoparticles need to escape from the endosomes before lysosomal degradation.[12] However, the efficiency of endosomal escape is often suboptimal. As a result, the development of novel intracellular delivery methods that are independent of endocytosis to enhance therapeutic efficiency has attracted considerable attention.

Several intracellular delivery methods *via* endocytosis-independent pathways, such as membrane fusion[13,14] and thiol-mediated uptake,[15–17] are considered powerful; however, these methods often require a combination with liposomal carriers or the chemical modification of drugs with cell-penetrating poly(disulfide)s. Methods that allow direct delivery of drugs into the cytoplasm without the need for encapsulation or chemical modifications have been reported. Futaki and co-workers reported a cationic amphiphilic peptide that can induce a ruffled appearance of the cell membrane and achieve the direct delivery of proteins into the cytoplasm;[18] however, it cannot currently be applied to the transfection of negatively charged nucleic acids. Physical techniques that induce cell-membrane disruption for intracellular delivery have been employed in nucleic acid delivery to cells due to their precision

[a] Department of Energy and Hydrocarbon Chemistry, Graduate School of Engineering, Kyoto University, Kyoto, 615-8510, Japan. E-mail: kojimiki@scl.kyoto-u.ac.jp, ohe@scl.kyoto-u.ac.jp
[b] Graduate School of Pharmaceutical Sciences, Osaka University, Osaka, 565-0871, Japan
[c] Center for Drug Design Research, National Institutes of Biomedical Innovation, Health and Nutrition, Osaka, 567-0085, Japan
[d] Institute for Open and Transdisciplinary Research Initiatives, Osaka University, Osaka, 565-0871, Japan
[e] Institute for Chemical Research, Kyoto University, Kyoto, 611-0011, Japan
[f] Research Institute for Interdisciplinary Science, Okayama University, Okayama, 700-8530, Japan

† Electronic supplementary information (ESI) available. See DOI: https://doi.org/10.1039/d3tb02956e

and controllability.[19] Nevertheless, mechanical methods are generally characterized by their low throughput and high degree of invasiveness, as well as the need for additional devices to physically puncture membranes, which hinders their widespread application in the field of pharmaceuticals.[20] García-López and co-workers pioneered a light-controllable molecular motor for directly opening lipid bilayer membranes.[21] Compared with mechanical transmembrane transport methods, the light-controllable molecular motor offers simpler experimental procedures. However, the light-controllable disturbance of the cell membrane induced by molecular motors is primarily utilized for ion transmembrane transport,[22–26] and is not generally applied to the cell-membrane permeability of even small molecules.

We herein report a light-controllable endocytosis-independent method for intracellular delivery of cell-impermeable molecules. Disturbing the cell membrane through such external stimuli allows for the high-throughput, direct delivery of drugs into the cytoplasm without the need for chemical modification. Under light irradiation, an amphiphilic light-triggered twistable molecule, **TPE-C-N**, can anchor to the cell membrane and induce continuous disturbance of the cell membrane (Fig. 1). Such disturbance loosens the packing of phospholipids, providing an opportunity for polar molecules to pass through the membrane and directly access the cytoplasm. Once light irradiation stops, the cell membrane spontaneously recovers its integrity, concluding the delivery process. This delivery system achieves: (i) selectivity in delivery through light-control, (ii) no permanent damage to the cell membrane, (iii) the ability to deliver molecules with any charge without requiring additional functionalization, and (iv) applicability to various cell lines. We have not only achieved intracellular delivery of negatively charged small molecule fluorescent dyes but have also successfully transported positively charged peptide drugs and negatively charged oligonucleotide drugs directly into the cytoplasm. The controllable disturbance of the cell membrane under external stimuli proposed in this study offers a novel design concept for drug delivery systems.

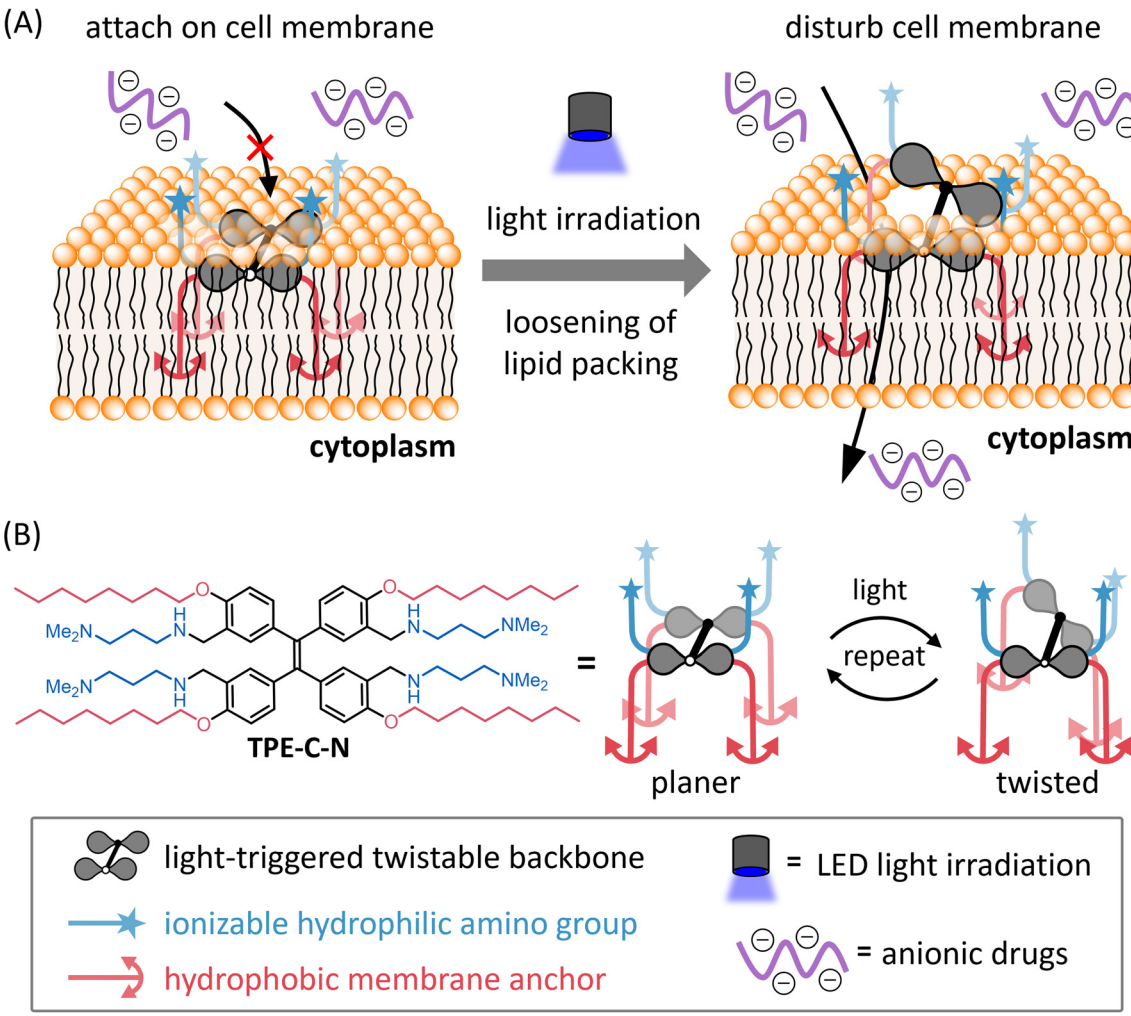

Fig. 1 (A) Schematic illustration of light-controllable intracellular delivery of anionic drugs mediated by **TPE-C-N**. (B) Molecular structure and the image of light-triggered twist of **TPE-C-N**.

Results and discussion

Molecular design

To achieve light-controllable disturbance of the cell membrane, the molecular backbone should undergo repetitive structural changes upon photoirradiation. Since the concept of aggregation-induced emission (AIE) was introduced by Tang and co-workers in 2001,[27] tetraphenylethene (TPE) has been well studied as a typical AIE molecule.[28] In the excited state, the π-bond becomes a biradical, leading to structural changes between planar and twisted configurations that consume excitation energy non-radiatively during photoirradiation. Based on the AIE effect, many reported fluorescent probes were designed to enhance their fluorescence by restricting the intramolecular motion of TPE.

Unlike the design concepts for AIE-based fluorescent probes, the aim of this molecular design is twofold: (i) to disturb the cell membrane by utilizing TPE backbone twisting and (ii) to achieve cell-membrane localization through the introduction of anchors. Therefore, we developed **TPE-C-N** for cell membrane disturbance by introducing positively charged substituents and lipophilic membrane anchors on the light-triggered twistable TPE backbone (Fig. 1(B)). Density functional theory (DFT) calculations were undertaken to predict the energy-minimized structures of the TPE derivative (**TPE-1**) in the ground and excited states (Fig. 2(A) and Fig. S1, ESI†). The results showed that the central double bond was essentially planar in the ground state, while it became twisted in the excited state. Such structural changes repeat constantly under photoirradiation, causing the substituents on the benzene

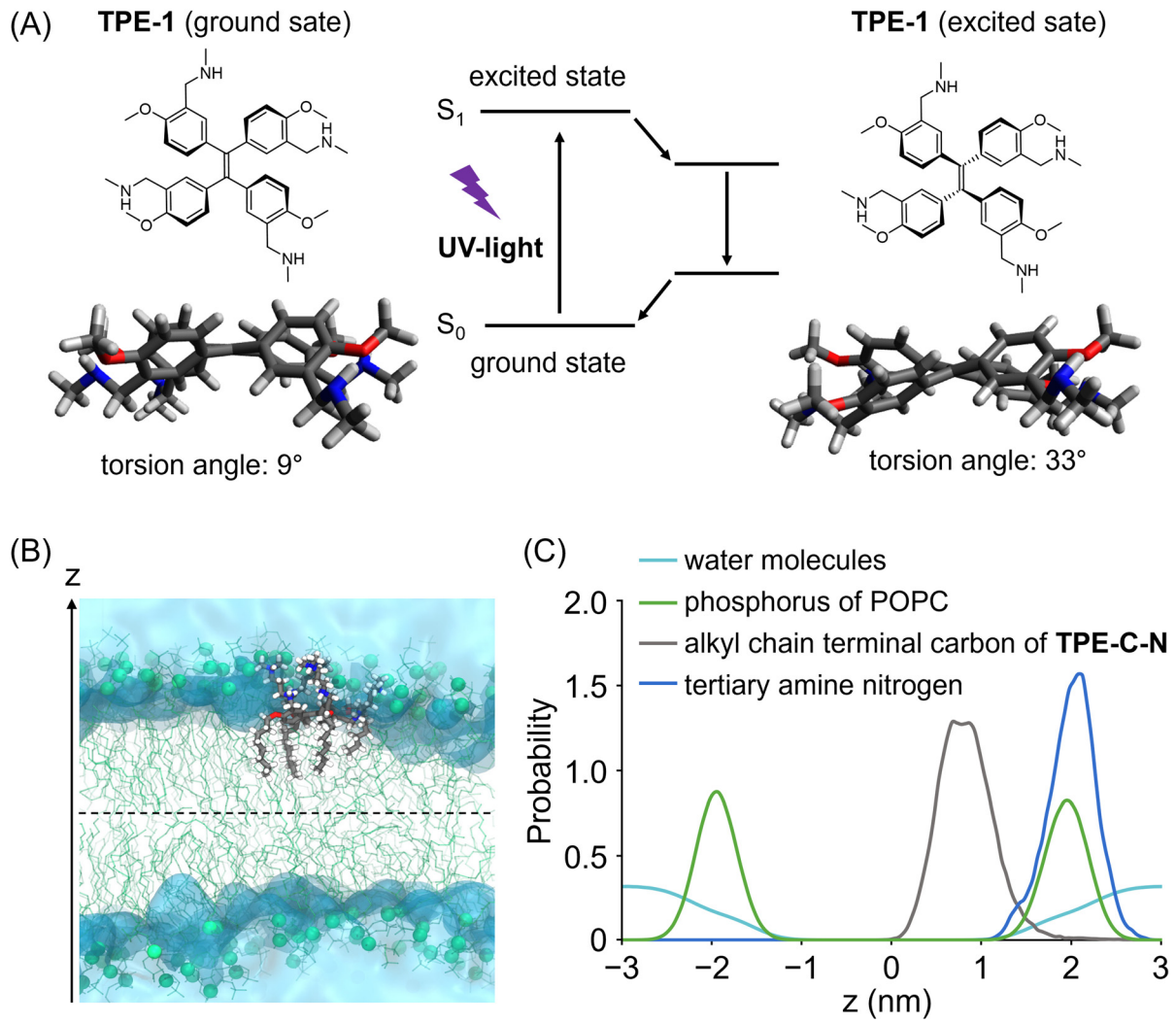

Fig. 2 (A) The energy-minimized geometries of TPE derivative (**TPE-1**) in the ground and excited states. For reducing calculation cost, the calculation of **TPE-C-N** without alkyl chains and amino groups were conducted. Calculation was carried out at M062X/6-31G(d,p) level. (B) Snapshot of **TPE-C-N** anchoring to the lipid bilayer in the brute force MD. POPC molecules are represented by green lines and spheres (phosphorous atoms). The blue, red, and white colours represent nitrogen, oxygen, and hydrogen atoms constituting **TPE-C-N**. The transparent cyan regions indicate water. (C) Probability distribution of phosphorus (green) of POPC, tertiary amine nitrogen (blue) and alkyl chain terminal carbon (grey) of **TPE-C-N**, and water molecules (cyan) along the bilayer normal, *z*.

rings at the *meta* and *para* positions to undergo relative displacement, thereby enabling the continuous disturbance of the cell membrane. To investigate the energy loss pathways upon molecular excitation, the photophysical properties of **TPE-C-N** were examined. In water/acetonitrile mixed solution, a strong absorbance at 300–400 nm was observed but almost no emission was detected (Fig. S2 and Tables S1, S2, ESI†). Although the quantum yield was not high (Φ_{FL} = 0.13), photoluminescence was detected in aqueous solution. Based on these properties, it was concluded that **TPE-C-N** does not aggregate strongly, and that its structure twists in aqueous solution.

To maintain a continuous disturbance of the cell membrane, **TPE-C-N** needs to efficiently accumulate and localize on the cell membrane. AIE fluorescent probes with positive charges and a good balance between hydrophilicity and hydrophobicity have been reported to be capable of localizing on the cell membrane.[29–32] Ionizable hydrophilic amino groups and hydrophobic membrane anchors are introduced on the TPE backbone to facilitate adsorption of the molecule onto the cell membrane (Fig. 1(B)). The interaction between **TPE-C-N** and the phospholipid bilayer was further examined through molecular dynamics (MD) simulation (Fig. 2(B), (C) and Fig. S3, ESI†). Palmitoyloleoyl phosphatidylcholine (POPC) was used to simulate the lipid bilayer. According to the calculated probability distribution of the selected atoms of **TPE-C-N** along the bilayer normal (the *z*-axis direction in Fig. 2(B)), the peak position of the phosphorus atoms of POPC in the upper leaflet of the bilayer was almost identical to that of the **TPE-C-N** tertiary amine nitrogen atoms (Fig. 2(C)). The terminal carbon atoms of the alkyl chain in **TPE-C-N** were distributed between the phosphorus peak position of POPC in the upper leaflet and the bilayer center. The results indicated that the amino groups and alkyl chains of **TPE-C-N** interact preferentially with the POPC lipid head-groups and tails, respectively. The MD simulation demonstrated that **TPE-C-N** was likely anchored to the lipid bilayers after adsorption to the upper leaflet surface.

Light-controllable enhancement of the cell-membrane permeability of anionic small molecules

Before assessing the **TPE-C-N**-mediated delivery efficiency under light irradiation, we evaluated the time-dependent cytotoxicity of the LED light used in this study (Fig. S4, ESI†). The results suggest that under the light intensity used in this study (10 mW cm^{-2}), UV irradiation for 5 to 10 min caused negligible cell damage. The efficiency of **TPE-C-N**-mediated transmembrane transport of charged molecules was investigated by incubating human lung cancer cell (A549) with a negatively charged fluorescent dye **Cy-5**, the molecular weight of which is around 1000 Da (Fig. 3(A)). Given that the cell-membrane permeability of **Cy-5** can be quantified through measurement of the intracellular fluorescence (FL) intensity, we employed a confocal laser scanning microscope (CLSM) to investigate whether **TPE-C-N** has the capacity to enhance the cell-membrane permeability of **Cy-5** under light irradiation. A549 cells were incubated with **TPE-C-N** in the dark for 5 min, followed by 5 min of incubation with **Cy-5** under LED light irradiation (Fig. 3(B) and Fig. S5, ESI†). In the absence of **TPE-C-N**, no detectable FL signal was observed in A549 cells. This can be attributed to the four negative charges on **Cy-5**, which prevents its penetration through the cell membrane. Under light irradiation, strong FL signals were detected in cells treated with **TPE-C-N**. The increased FL intensity indicates the enhanced cell-membrane permeability of **Cy-5**. To further quantify the intracellular delivery of **Cy-5**, we calculated the unit area average FL intensity (relative FL intensity) in the CLSM images from three independent experiments (Fig. 3(C)). **TPE-C-N** significantly improved the cell-membrane permeability of **Cy-5** under light irradiation. It is worth noting that even in the absence of light, **TPE-C-N** increased the FL intensity of **Cy-5** in A549 cells slightly. Analysis of their CLSM images in the dark control group revealed that the FL signal was localized primarily at the cell membrane (Fig. 3(B); dark, **TPE-C-N** (+)). This is due to the amphiphilic nature of **TPE-C-N**, which carries ionizable cations, facilitating its electrostatic interaction with **Cy-5** and enhancing the lipophilicity of **Cy-5**. Co-localization experiments with **TPE-C-N** and **Cy-5** in A549 cells showed that the blue fluorescence from **TPE-C-N** and the red fluorescence from **Cy-5** were both localized at the cell membrane (Fig. 3(D), dark). This result reveals that **TPE-C-N** does not effectively disturb the cell membrane in the absence of LED light, and that **Cy-5** remains trapped in the cell membrane and fails to access the cytoplasm. During the intracellular delivery of **Cy-5** under light irradiation, **TPE-C-N** remains localized on the cell membrane, while **Cy-5** efficiently accesses the cytoplasm (Fig. 3(D), light). It was proven that electrostatic interaction between **TPE-C-N** and **Cy-5** is negligible for the light-controlled delivery process; instead, **TPE-C-N** promotes the intracellular delivery of **Cy-5** by disturbing the cell membrane. To investigate how the residual **TPE-C-N** is removed from the cells, we monitored the changes in **TPE-C-N** fluorescence signals after light-mediated delivery (Fig. S6, ESI†). The results show that the fluorescence signal of **TPE-C-N** was almost undetectable 6 h later, indicating that **TPE-C-N** is gradually removed from the cells.

To further investigate the roles played by the hydrophilic amino group and the lipophilic alkyl chain of **TPE-C-N** in the promotion of **Cy-5** delivery efficiency, we synthesized control molecules **TPE-N** and **TPE-C** (Fig. 3(A)). Both **TPE-N** and **TPE-C** possess the same light-triggered twistable TPE backbone as **TPE-C-N**; however, **TPE-N** lacks alkyl chains, and **TPE-C** lacks ionizable amino groups. The promoting effect of **TPE-N**, **TPE-C**, and **TPE-C-N** on the cell-membrane permeability of **Cy-5** under light irradiation was assessed by flow cytometric analysis (Fig. S7, ESI†). Cells were incubated with **TPE**s in the dark for 5 min, then incubated with **Cy-5** for 10 min under light irradiation. The ratio of cells stained with **Cy-5** to the total number of cells was determined from flow cytometric analysis, denoted as gate%. The gate% serves as a metric for measuring **Cy-5** delivery efficiency (Fig. 3(E)). **TPE-N** and **TPE-C** did not enhance the gate% of **Cy-5**. In other words, **TPE-N** and **TPE-C** were incapable of promoting intracellular **Cy-5** delivery by disturbing the cell membrane. Conversely, **TPE-C-N** significantly improved the delivery efficiency of **Cy-5** under light

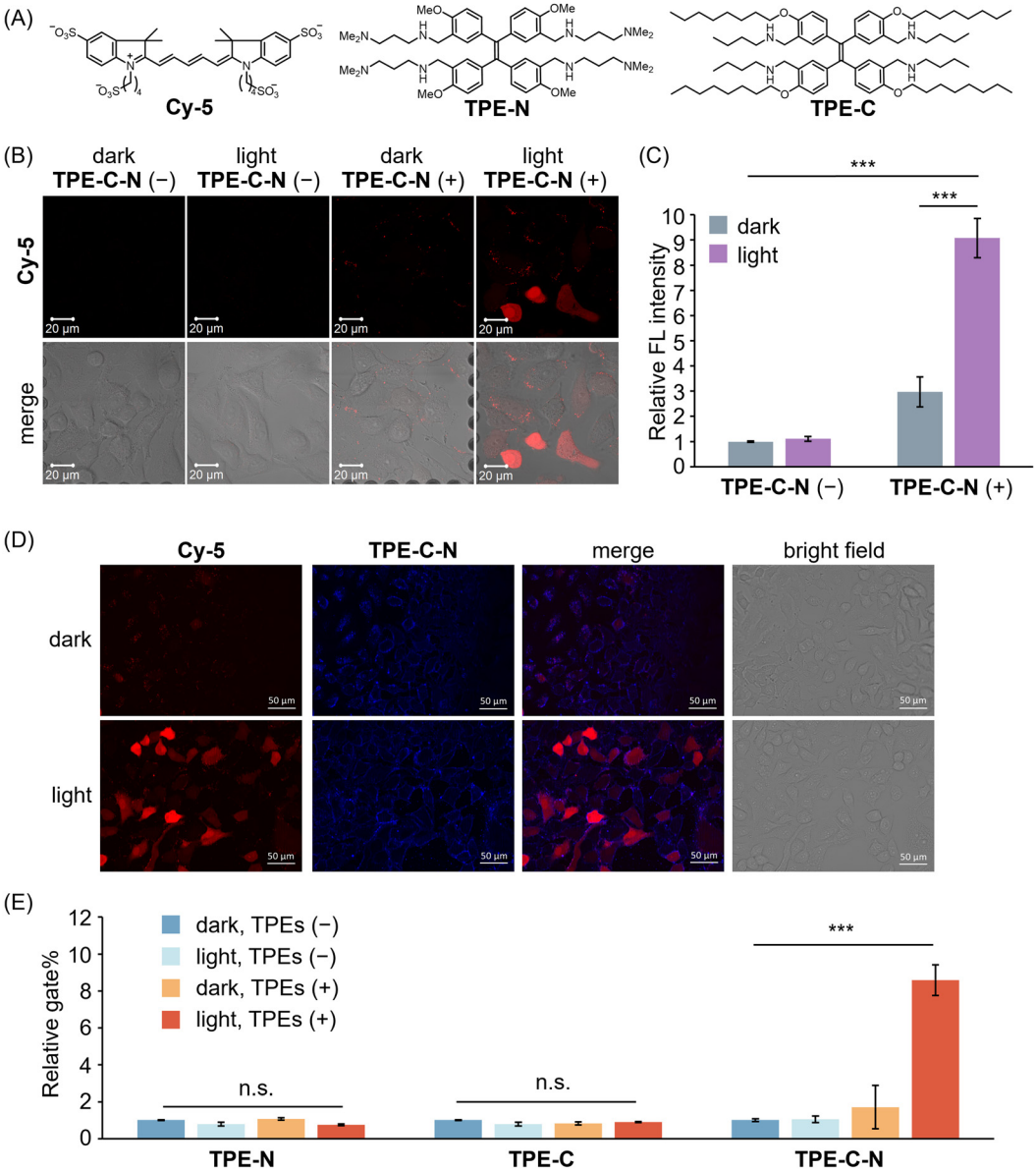

Fig. 3 (A) Molecular structures of **Cy-5**, **TPE-N**, and **TPE-C**. (B) CLSM images of A549 cells incubated with **Cy-5** for 5 min under different treatments. λ_{ex} = 633 nm, λ_{det} = 647–759 nm. Scale bar: 20 μm. (C) Relative FL intensity calculated based on CLSM images (Fig. 3(B) shows the representative image) obtained from three independent experiments (n = 3). (D) Fluorescence images of A549 cells incubated with **Cy-5** in the presence of **TPE-C-N** in dark or under LED light irradiation. Red channel (**Cy-5**): λ_{ex} = 600/60 nm, λ_{det} = 700/75 nm. Blue channel (**TPE-C-N**): λ_{ex} = 350/50 nm, λ_{det} = 500/40 nm. Scale bar: 50 μm. (E) Relative gate% calculated from flow cytometric analysis of A549 cells respectively treated with **TPE-N**, **TPE-C**, and **TPE-C-N**, and then incubated with **Cy-5** for 10 min. Results are calculated from three samples (n = 3). General conditions: **TPE**s (+): 10 μM; **Cy-5**: 10 μM; LED light irradiation: 365 nm (10 mW cm^{-2}). Results are presented as the mean ± standard deviation. Student's t-test: n.s. = not significant, *** $p < 0.001$.

irradiation. To understand why **TPE-N** and **TPE-C** fail to enhance the delivery efficiency of **Cy-5**, fluorescence microscopy images of cells that were incubated with **TPE-N** and **TPE-C**, respectively, were recorded (Fig. S8, ESI†). It was found that neither **TPE-N** nor **TPE-C** localized at the cell membrane; instead, they entered the cytoplasm directly. This indicates that the ionizable amino group and the hydrophobic alkyl chain play crucial roles in maintaining the consistent disturbance of the cell membrane under light irradiation.

Self-recovery of cell membrane integrity after light irradiation

Hydrophobic forces drive the efficient self-assembly of lipid bilayers into a two-dimensional fluid,[33] thereby facilitating the self-annealing of defects within the membrane plane to recover cell membrane integrity. The self-recovery capability of the cell membrane after the disturbance of **TPE-C-N** was investigated by using the membrane-impermeable fluorescent dye propidium iodide (PI). A549 cells treated with **TPE-C-N** under light irradiation were cultured in medium for 15 min before adding

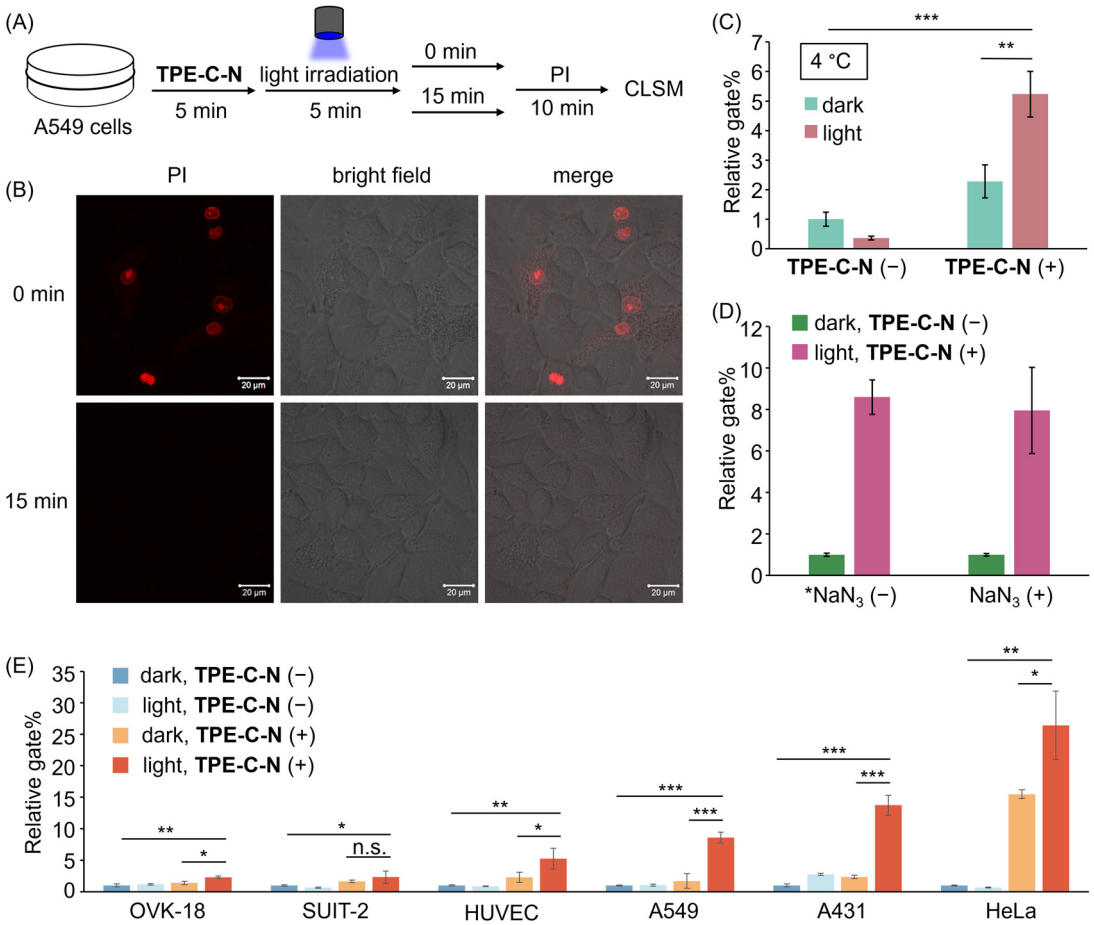

Fig. 4 (A) Schematic diagram of PI penetration experiments. (B) CLSM images of A549 cells treated with **TPE-C-N** under LED light irradiation for 5 min, and then incubated in medium for 0 min and 15 min before the addition of PI (10 μg mL^{-1}). λ_{ex} = 488 nm, λ_{det} = 551–697 nm. Scale bar: 20 μm. (C) Relative gate% calculated from flow cytometric analysis of A549 cells treated with **Cy-5** for 10 min under different treatments at 4 °C. (D) Relative gate% calculated from flow cytometric analysis of A549 cells treated with **Cy-5** under different treatments. *NaN_3 (−) data are obtained from Fig. 3(E). NaN_3 (+): 10 mM. (E) Relative gate% calculated from flow cytometric analysis of OVK-18, SUIT-2, HUVEC, A549, A431, and HeLa cells treated with **Cy-5** for 10 min under different treatments. General conditions: **TPE-C-N** (+): 10 μM; **Cy-5**: 10 μM; LED light irradiation: 365 nm (10 mW cm^{-2}). Results are presented as the mean ± standard deviation of three samples (n = 3). Student's t-test: n.s. = not significant, * $p < 0.05$, ** $p < 0.01$, *** $p < 0.001$.

PI (Fig. 4(A)). As a control experiment, another group of **TPE-C-N**-treated A549 cells were immediately treated with PI after light irradiation. In the control experiment, the fluorescence from PI was detected at the nucleus of cells, indicating that the cell membrane remained permeable to PI just after light irradiation (Fig. 4(B)). However, after a 15 min self-recovery period, the integrity of the cell membrane had been fully restored, preventing the transport of PI across the membrane. We assessed the cell viability of A549 cells, which were cultured in medium for 30 min after light irradiation, using the CCK-8 assay (Fig. S9, ESI†). The results showed that **TPE-C-N** and light did not affect cell viability. These results support the conclusion that **TPE-C-N**-promoted cell membrane disturbance under light irradiation is transient and does not lead to permanent damage to the cell membrane.

Intracellular delivery of anionic dyes after inhibiting endocytosis

To verify that **TPE-C-N** facilitates the direct access of charged molecules to the cytoplasm in an endocytosis-independent manner, we inhibited cellular endocytosis through low-temperature treatment. After pretreating cells at 4 °C for 15 min, the cell-membrane permeability of **Cy-5** was evaluated using flow cytometry (Fig. S10, ESI†). The gate% for **Cy-5** delivery efficiency indicated that, irrespective of whether endocytosis was inhibited, **TPE-C-N** significantly enhances the intracellular delivery efficiency of **Cy-5** under light irradiation (Fig. 4(C)). This strongly supports the conclusion that the light-controllable cellular internalization induced by **TPE-C-N** is endocytosis-independent.

Intracellular delivery of anionic dyes in the presence of singlet oxygen quencher

Photochemical internalization is a technique involving the release of endocytosed macromolecules into the cytoplasm upon light activation.[34] It relies on photosensitizers within endocytic vesicles, which, when exposed to light, produce highly reactive singlet oxygen ($^1O_2$).[35] Singlet oxygen has been shown to irreversibly alter lipid membrane structure and

increase membrane permeability.[36,37] To explore whether the **TPE-C-N**-induced disturbance of the cell membrane under light irradiation is associated with the generation of $^1O_2$, we conducted cell delivery experiments of **Cy-5** using A549 cells pretreated with the $^1O_2$ quencher sodium azide (NaN_3).[38] The cell membrane permeability of **Cy-5** was evaluated *via* flow cytometric analysis (Fig. 4(D) and Fig. S11, ESI†). The presence of **TPE-C-N** enhanced the delivery of **Cy-5** to NaN_3-pretreated cells under light irradiation. Compared with cells that were not treated with NaN_3, the delivery efficiency promoted by **TPE-C-N** was comparable to those treated with $^1O_2$ quencher. This result strongly demonstrates that this **TPE-C-N**-mediated light-controllable intracellular delivery is a novel drug delivery method that is distinct from photochemical internalization. In addition to serving as a $^1O_2$ quencher, NaN_3 is also a well-known mitochondrial respiration inhibitor, capable of blocking energy-dependent endocytosis.[39] The presence of NaN_3 did not affect the intracellular delivery of **Cy-5**, which is consistent with the results from low-temperature inhibition of endocytosis, as shown in the previous section.

Applicability to various cell lines

The transmembrane delivery of **Cy-5** with the assistance of **TPE-C-N** towards different cell lines was investigated by flow cytometric analysis. Commonly used cancer cell lines were selected: human ovarian endometrioid adenocarcinoma cell (OVK-18), human pancreatic adenocarcinoma cell (SUIT-2), human epidermoid carcinoma cell (A431), and human cervical cancer cell (HeLa); along with healthy human umbilical vein endothelial cell (HUVEC). After treating various cell types with **TPE-C-N**, the intracellular delivery efficiency of **Cy-5** under light irradiation was evaluated through flow cytometric analysis (Fig. 4(E) and Fig. S12, ESI†). In all tested cell lines, whether cancerous or healthy, the light-controllable **TPE-C-N**-induced promotion of intracellular delivery efficiency was confirmed. To investigate whether the light-controllable delivery process would cause sustained cytotoxicity to HeLa cells, which showed the highest delivery efficiency, the cell viability of HeLa cells treated with **TPE-C-N** under light irradiation and then further incubated in medium for 24 h was studied using the CCK-8 assay (Fig. S13, ESI†). The results showed that the remaining **TPE-C-N** does not cause sustained damage to the normal functions of HeLa cells. Notably, whereas high delivery efficiency was exhibited by **TPE-C-N** in A431 cells, the most common transfection reagent, lipofectamine,[40] demonstrated inefficient delivery. This further suggests the vast potential of **TPE-C-N** in the field of drug delivery.

Light-controllable enhancement of the cell-membrane permeability of cationic peptides

TPE-C-N significantly enhances the intracellular uptake efficiency of negatively charged molecules, which encouraged us to further investigate whether **TPE-C-N** can facilitate the intracellular delivery of positively charged molecules. Arginine-rich cell-penetrating peptides, such as octaarginine (R8), carry a positive charge at physiological pH and are commonly used for intracellular delivery of bioactive molecules.[41] Fluorescein isothiocyanate (FITC) was employed as a fluorescent tag to label R8 (FITC-R8), enabling the evaluation of the intracellular delivery efficiency of R8 through the intensity of FL signals. After incubating A549 cells with **TPE-C-N** for 5 min, cells were subsequently cultured with FITC-R8 for 5 min under light irradiation (Fig. 5(A) and Fig. S14, ESI†). The positively charged FITC-R8 struggled to permeate the cell membrane and access the cytoplasm in the absence of **TPE-C-N**. In the presence of amphiphilic **TPE-C-N**, the intracellular delivery efficiency of FITC-R8 exhibited a slight improvement even without light irradiation. This phenomenon was also observed in the intracellular delivery of **Cy-5**. In the presence of **TPE-C-N**, FITC-R8 crossed the cell membrane efficiently and dispersed directly throughout the entire cell under light irradiation, indicating that FITC-R8 can access the cytoplasm through an endocytosis-independent pathway. The relative FL intensity calculated from three independent experiments provides a more intuitive demonstration of the promoting effect by **TPE-C-N** on the light-controllable intracellular delivery of FITC-R8, the molecular weight of which is around 1500 Da (Fig. 5(B)).

We further investigated whether the light-controllable intracellular delivery induced by **TPE-C-N** can be applied to larger peptide-based drugs. It is known that the pro-apoptotic domain peptide (PAD, d(KLAKLAK)$_2$-amide, comprised of all D-amino acids) induces apoptosis when delivered into cells.[42] Hence, the intracellular delivery efficiency of R8 modified PAD (R8-PAD, MW *ca.* 3000 Da) can be assessed through cell viability. After treatment with **TPE-C-N**, one plate of cells continued to be cultured with R8-PAD (Fig. 5(C); R8-PAD (+)), while a second served as a control group (Fig. 5(C); R8-PAD (−)). After 5 min light irradiation, the cell viabilities of **TPE-C-N**- and R8-PAD-treated cells were assessed using the CCK-8 assay. Cells that were not cultured with R8-PAD maintained nearly 100% viability, regardless of **TPE-C-N** treatment and light irradiation. R8-PAD exhibited mild cytotoxicity in cells without **TPE-C-N** treatment, and this cytotoxicity increased significantly in cells treated with **TPE-C-N** irradiated by LED light. Considering that R8-PAD induces apoptosis only after entering the cytoplasm, the increase in cytotoxicity is attributed to the enhanced intracellular delivery efficiency.

Light-controllable enhancement of the cell-membrane permeability of anionic oligonucleotides

Gene therapy using antisense oligonucleotides (ASOs) hold immense promise for treating various diseases, including cancer, genetic disorders, and viral infections, as it induces targeted RNA cleavage mediated by ribonuclease H through binding to the target RNA within cells.[43,44] However, the permeability of oligonucleotides into cells is extremely low due to their negative charges. Considering that nucleic acid drugs must be delivered to the cytoplasm to take effect, it can be anticipated that the endocytosis-independent pathways mediated by **TPE-C-N** hold great potential in advancing gene therapy. Metastasis-associated lung adenocarcinoma transcript 1 (*MALAT1*) is a long noncoding RNA that plays a crucial role in

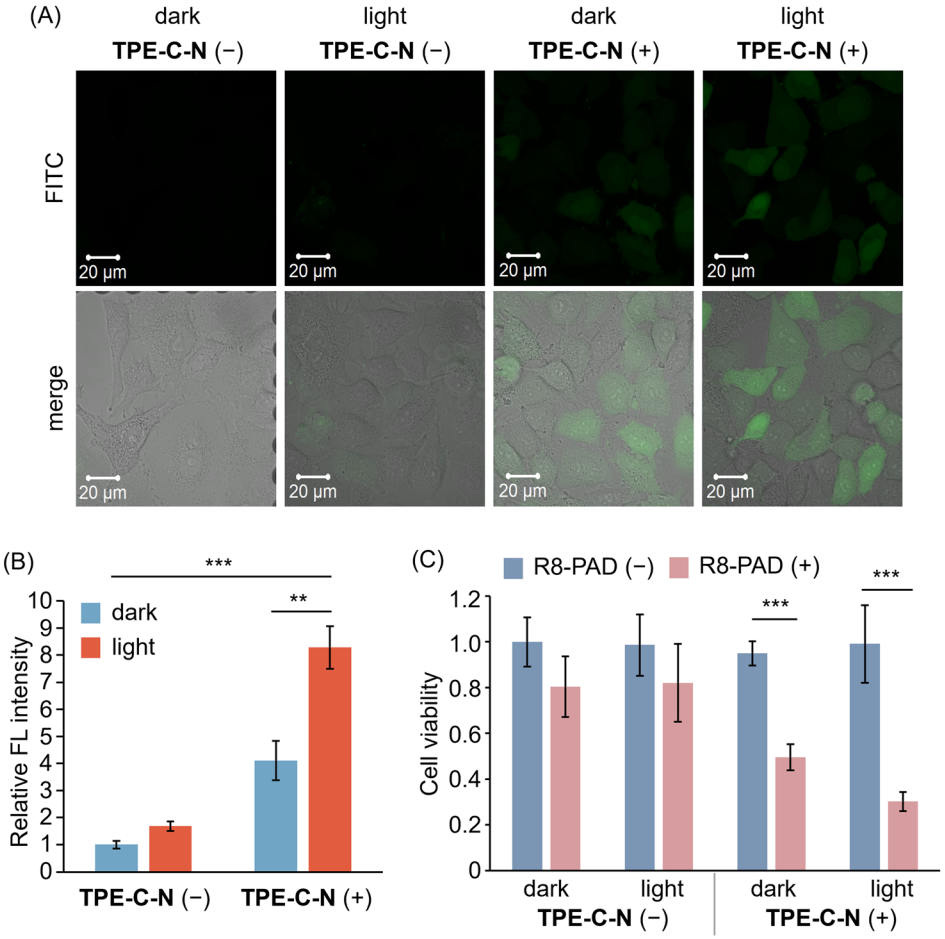

Fig. 5 (A) CLSM images of A549 cells incubated with FITC-R8 (10 μM in PBS) for 5 min under different treatments. λ_{ex} = 488 nm, λ_{det} = 493–630 nm. Scale bar: 20 μm. (B) Relative FL intensity calculated based on CLSM images (Fig. 5(A) shows the representative image) obtained from three independent experiments (n = 3). (C) Cell viability of A549 cells with (blue) or without (pink) the treatment of R8-PAD. R8-PAD (+): 5 μM. Results are obtained from five samples (n = 5). General conditions: **TPE-C-N** (+): 10 μM; LED light irradiation: 365 nm (10 mW cm^{-2}). Results are presented as the mean ± standard deviation. Student's t-test: ** $p < 0.01$, *** $p < 0.001$.

lung cancer metastasis and cell migration.[45] In this study, the MALAT1-ASO, designed to reduce the expression level of *MALAT1*, was used to investigate whether nucleic acid drugs with a molecular weight of approximately 5000 Da could be delivered into MIA PaCa-2-Luc cells *via* the light-controllable pathway mediated by **TPE-C-N**. Knockdown of *MALAT1* RNA expression allows for the evaluation of the MALAT1-ASO intracellular delivery efficiency. After light irradiation, the **TPE-C-N**- and MALAT1-ASO-treated MIA PaCa-2-Luc cells were washed and incubated in medium containing MALAT1-ASO for 30 min. Subsequently, cells were incubated in medium without MALAT1-ASO for 3.5 h. No significant knockdown of *MALAT1* RNA expression was observed in control experiments with cells transfected with negative control ASO (NEG-ASO) or in control experiments without light irradiation (Fig. S15, ESI†). In contrast, under light irradiation, **TPE-C-N** reduced *MALAT1* RNA expression level by 11% (Fig. 6). This suggests that the light-controllable intracellular delivery method mediated by **TPE-C-N** allows for the direct transportation of MALAT1-ASO into the cytoplasm. Compared with commercial transfection reagents,

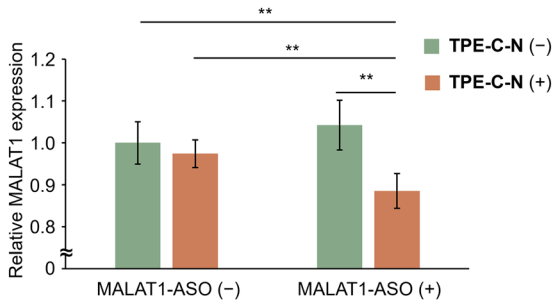

Fig. 6 Relative expression level of *MALAT1* in MIA PaCa-2-Luc cells with different treatments under light irradiation. MALAT1-ASO: 480 nM; **TPE-C-N**: 10 μM; LED light irradiation: 365 nm (10 mW cm^{-2}), 10 min. Results are presented as the mean ± standard deviation of eight samples (n = 8). Student's t-test; ** $p < 0.01$.

TPE-C-N-mediated light-controllable intracellular delivery has a shorter incubation time and is applicable to cell lines where commercial reagents are inefficient, making it a promising alternative for transfection.

Conclusion

We have developed **TPE-C-N** as a light-triggered twistable molecule for effective intracellular delivery of cell-impermeable therapeutic compounds ranging in molecular weight from 1000 to 5000 Da through an endocytosis-independent pathway. The cationic ionizable amino group and the hydrophobic alkyl chain ensure that **TPE-C-N** can effectively accumulate on the cell membrane, while the TPE backbone allows **TPE-C-N** to continuously disturb the cell membrane under light irradiation. Such disturbance does not cause permanent damage to the cell membrane, and we have demonstrated that the membrane can self-recover its integrity after light irradiation. When cellular endocytosis was inhibited by low-temperature treatment, **TPE-C-N** was still able to significantly enhance the intracellular delivery of negatively charged fluorescent dyes under light irradiation, suggesting that this delivery method is indeed endocytosis-independent. We also investigated the effectiveness of this light-controllable intracellular delivery method in different cell lines. The results show that, although the extent varied, the delivery efficiency of cell-impermeable compounds was improved in all tested cell lines. The novel intracellular delivery method proposed in this study is applicable to transporting molecules with any charge, without the need for additional chemical modifications, and does not require inefficient endosomal escape. Although addressing the issue of short-wavelength light irradiation remains a challenge in developing the light-controllable intracellular delivery method into a mature technology suitable for *in vivo* applications, the new intracellular delivery method proposed in this study is capable of transporting any charged molecule without the need for additional chemical modifications and does not require the inefficient endosomal escape. It is foreseeable that this research will inject new vitality into the development of drug delivery systems.

Author contributions

K. M., T. O., S. O., H. H., S. F. and S. A. conceived the study. W. H., K. M. and H. M. prepared and characterized TPEs. W. H., K. M. and H. M. performed general cell experiments. W. H., K. M., Y. Kawaguchi, H. H. and S. F. carried out the flow cytometric analysis. T. O., H. Y., Y. Kasahara, S. O., W. H. and K. M. performed cell experiments of ASO. Y. M. and W. S. carried out the MD simulation. K. M. and K. O. supervised research. W. H., K. M. and K. O. wrote the manuscript. All authors reviewed and approved the manuscript.

Conflicts of interest

There are no conflicts to declare.

Acknowledgements

This work was supported by JSPS KAKENHI grant number JP23KJ1297. K. M. appreciates the financial support from The Asahi Glass Foundation and The Uehara Memorial Foundation. W. H. thanks for the financial support from Otsuka Toshimi Scholarship Foundation. We thank Prof. Kazuo Tanaka and Prof. Masayuki Gon for assistance with fluorescence lifetime measurement. Computations were performed at the supercomputer facilities of the Institute for Chemical Research, Kyoto University, the Research Center for Computational Science, Okazaki (project: 23-IMS-C095) and the Institute for Solid State Physics, the University of Tokyo.

References

1 Q. Sun, Z. Zhou, N. Qiu and Y. Shen, *Adv. Mater.*, 2017, **29**, 1606628.
2 J. Lindberg, J. Nilvebrant, P.-Å. Nygren and F. Lehmann, *Molecules*, 2021, **26**, 6042.
3 R. Kole, A. R. Krainer and S. Altman, *Nat. Rev. Drug Discovery*, 2012, **11**, 125–140.
4 K. Siva, G. Covello and M. A. Denti, *Nucleic Acid Ther.*, 2014, **24**, 69–86.
5 A. Wittrup and J. Lieberman, *Nat. Rev. Genet.*, 2015, **16**, 543–552.
6 O. Khorkova and C. Wahlestedt, *Nat. Biotechnol.*, 2017, **35**, 249–263.
7 M. Matsui and D. R. Corey, *Nat. Rev. Drug Discovery*, 2017, **16**, 167–179.
8 C. A. Lipinski, F. Lombardo, B. W. Dominy and P. J. Feeney, *Adv. Drug Delivery Rev.*, 2001, **46**, 3–26.
9 J. Buck, P. Grossen, P. R. Cullis, J. Huwyler and D. Witzigmann, *ACS Nano*, 2019, **13**, 3754–3782.
10 R. Tenchov, R. Bird, A. E. Curtze and Q. Zhou, *ACS Nano*, 2021, **15**, 16982–17015.
11 D. W. Pack, A. S. Hoffman, S. Pun and P. S. Stayton, *Nat. Rev. Drug Discovery*, 2005, **4**, 581–593.
12 S. Du, S. S. Liew, L. Li and S. Q. Yao, *J. Am. Chem. Soc.*, 2018, **140**, 15986–15996.
13 M. Segel, B. Lash, J. Song, A. Ladha, C. C. Liu, X. Jin, S. L. Mekhedov, R. K. Macrae, E. V. Koonin and F. Zhang, *Science*, 2021, **373**, 882–889.
14 J. Yang, J. Tu, G. E. M. Lamers, R. C. L. Olsthoorn and A. Kros, *Adv. Healthcare Mater.*, 2017, **6**, 1700759.
15 G. Gasparini, E. K. Bang, G. Molinard, D. V. Tulumello, S. Ward, S. O. Kelley, A. Roux, N. Sakai and S. Matile, *J. Am. Chem. Soc.*, 2014, **136**, 6069–6074.
16 D. Abegg, G. Gasparini, D. G. Hoch, A. Shuster, E. Bartolami, S. Matile and A. Adibekian, *J. Am. Chem. Soc.*, 2017, **139**, 231–238.
17 N. Chuard, A. I. Poblador-Bahamonde, L. Zong, E. Bartolami, J. Hildebrandt, W. Weigand, N. Sakai and S. Matile, *Chem. Sci.*, 2018, **9**, 1860–1866.
18 M. Akishiba and S. Futaki, *Mol. Pharmaceutics*, 2019, **16**, 2540–2548.
19 M. P. Stewart, A. Sharei, X. Ding, G. Sahay, R. Langer and K. F. Jensen, *Nature*, 2016, **538**, 183–192.

20 A. Fu, R. Tang, J. Hardie, M. E. Farkas and V. M. Rotello, *Bioconjugate Chem.*, 2014, **25**, 1602–1608.
21 V. García-López, F. Chen, L. G. Nilewski, G. Duret, A. Aliyan, A. B. Kolomeisky, J. T. Robinson, G. Wang, R. Pal and J. M. Tour, *Nature*, 2017, **548**, 567–572.
22 W.-Z. Wang, L.-B. Huang, S.-P. Zheng, E. Moulin, O. Gavat, M. Barboiu and N. Giuseppone, *J. Am. Chem. Soc.*, 2021, **143**, 15653–15660.
23 H. Yang, J. Yi, S. Pang, K. Ye, Z. Ye, Q. Duan, Z. Yan, C. Lian, Y. Yang, L. Zhu, D.-H. Qu and C. Bao, *Angew. Chem., Int. Ed.*, 2022, **61**, e202204605.
24 J. Shen, C. Ren and H. Zeng, *Acc. Chem. Res.*, 2022, **55**, 1148–1159.
25 S. J. Wezenberg, L.-J. Chen, J. E. Bos, B. L. Feringa, E. N. W. Howe, X. Wu, M. A. Siegler and P. A. Gale, *J. Am. Chem. Soc.*, 2022, **144**, 331–338.
26 A. L. Santos, D. Liu, A. K. Reed, A. M. Wyderka, A. V. Venrooy, J. T. Li, V. D. Li, M. Misiura, O. Samoylova, J. L. Beckham, C. Ayala-Orozco, A. B. Kolomeisky, L. B. Alemany, A. Oliver, G. P. Tegos and J. M. Tour, *Sci. Adv.*, 2022, **8**, eabm2055.
27 J. Luo, Z. Xie, J. W. Y. Lam, L. Cheng, H. Chen, C. Qiu, H. S. Kwok, X. Zhan, Y. Liu, D. Zhu and B. Z. Tang, *Chem. Commun.*, 2001, 1740–1741.
28 J. Mei, N. L. C. Leung, R. T. K. Kwok, J. W. Y. Lam and B. Z. Tang, *Chem. Rev.*, 2015, **115**, 11718–11940.
29 F. Wang, P.-Y. Ho, C. Kam, Q. Yang, J. Liu, W. Wang, E. Zhao and S. Chen, *Aggregate*, 2023, **4**, e312.
30 Y. Hu, S.-Y. Yin, W. Liu, Z. Li, Y. Chen and J. Li, *Aggregate*, 2023, **4**, e256.
31 W. Zhang, Y. Huang, Y. Chen, E. Zhao, Y. Hong, S. Chen, J. W. Y. Lam, Y. Chen, J. Hou and B. Z. Tang, *ACS Appl. Mater. Interfaces*, 2019, **11**, 10567–10577.
32 Y. Li, Y. Wu, J. Chang, M. Chen, R. Liu and F. Li, *Chem. Commun.*, 2013, **49**, 11335–11337.
33 G. Vereb, J. Szöllősi, J. Matkó, P. Nagy, T. Farkas, L. Vígh, L. Mátyus, T. A. Waldmann and S. Damjanovich, *Proc. Natl. Acad. Sci. U. S. A.*, 2003, **100**, 8053–8058.
34 K. Berg, P. K. Selbo, L. Prasmickaite, T. E. Tjelle, K. Sandvig, J. Moan, G. Gaudernack, Ø. Fodstad, S. Kjølsrud, H. Anholt, G. H. Rodal, S. K. Rodal and A. Høgset, *Cancer Res.*, 1999, **59**, 1180–1183.
35 R. C. Richmond and J. A. O'Hara, *Photochem. Photobiol.*, 1993, **57**, 291–297.
36 A. G. Ayuyan and F. S. Cohen, *Biophys. J.*, 2006, **91**, 2172–2183.
37 C. K. Haluska, M. S. Baptista, A. U. Fernandes, A. P. Schroder, C. M. Marques and R. Itri, *Biochim. Biophys. Acta, Biomembr.*, 2012, **1818**, 666–672.
38 J. Zhang, R. Zhang, K. Liu, Y. Li, X. Wang, X. Xie, X. Jiao and B. Tang, *Chem. Commun.*, 2021, **57**, 8320–8323.
39 M. W. Bowler, M. G. Montgomery, A. G. W. Leslie and J. E. Walker, *Proc. Natl. Acad. Sci. U. S. A.*, 2006, **103**, 8646–8649.
40 B. Dalby, S. Cates, A. Harris, E. C. Ohki, M. L. Tilkins, P. J. Price and V. C. Ciccarone, *Methods*, 2004, **33**, 95–103.
41 K. Sakamoto, K. Aburai, T. Morishita, K. Sakai, H. Sakai, M. Abe, I. Nakase and S. Futaki, *Chem. Lett.*, 2012, **41**, 1078–1080.
42 S. Pujals, H. Miyamae, S. Afonin, T. Murayama, H. Hirose, I. Nakase, K. Taniuchi, M. Umeda, K. Sakamoto, A. S. Ulrich and S. Futaki, *ACS Chem. Biol.*, 2013, **8**, 1894–1899.
43 L. Naldini, *Nature*, 2015, **526**, 351–360.
44 C. W. Peterson, P. Younan, K. R. Jerome and H.-P. Kiem, *Gene Ther.*, 2013, **20**, 695–702.
45 T. Gutschner, M. Hämmerle and S. Diederichs, *J. Mol. Med.*, 2013, **91**, 791–801.